Maximizing the Efficiency of Multienzyme Process by Stoichiometry Optimization

Pavel Dvorak,[a, b] Nagendra P. Kurumbang,[a] Jaroslav Bendl,[a, b, c] Jan Brezovsky,[a] Zbynek Prokop,[a, b] and Jiri Damborsky*[a, b]

Multienzyme processes represent an important area of biocatalysis. Their efficiency can be enhanced by optimization of the stoichiometry of the biocatalysts. Here we present a workflow for maximizing the efficiency of a three-enzyme system catalyzing a five-step chemical conversion. Kinetic models of pathways with wild-type or engineered enzymes were built, and the enzyme stoichiometry of each pathway was optimized. Mathematical modeling and one-pot multienzyme experiments provided detailed insights into pathway dynamics, enabled the selection of a suitable engineered enzyme, and afforded high efficiency while minimizing biocatalyst loadings. Optimizing the stoichiometry in a pathway with an engineered enzyme reduced the total biocatalyst load by an impressive 56%. Our new workflow represents a broadly applicable strategy for optimizing multienzyme processes.

In vitro multienzyme processes have great potential for the biosynthesis of fine and bulk chemicals, for bioremediation and biosensing.[1] Studies on two-enzyme systems dominate the literature, but systems of three,[2] four,[3] and even twelve[4] or thirteen[5] enzymes are known. Multienzyme systems are superior to single-enzyme biocatalysis in that they can catalyze more-complex synthetic schemes. In vitro multienzyme networks enable simpler process control than analogous in vivo systems and suffer less from reactant toxicity.[6] However, in both system types reaction bottlenecks often arise from imbalanced enzyme properties.

Protein engineering is often used to improve the catalytic properties and stability of enzymes.[7] Many engineered enzymes can be used in multienzyme processes, but methods for predicting their impact on productivity are lacking. Kinetic modeling is essential for analyzing enzymatic reactions and can enable their rational optimization.[1c, 8] However, there are only few accurate kinetic models of in vitro multienzyme systems.[2, 3, 5, 9] Available models rarely have experimental support, and their use in optimizing processes with engineered enzymes has not been adequately explored.

The aim of this study was to develop a workflow for optimizing multienzyme processes by using kinetic modeling to predict the effects of varying enzyme stoichiometry and employing available engineered enzymes. Our model system (Scheme 1) was a synthetic metabolic pathway for the five-step biotransformation of toxic industrial waste product 1,2,3-trichloropropane (TCP) into glycerol (GLY).[10] This pathway has been previously assembled inside living cells[11] and is based on haloalkane dehalogenase DhaA from *Rhodococcus rhodochrous* NCIMB 13064,[12] haloalcohol dehalogenase HheC from *Agrobacterium radiobacter* AD1,[13] and epoxide hydrolase EchA from *Agrobacterium radiobacter* AD1.[14] Herein, three DhaA variants were assessed: 1) wild-type DhaA, and the previously constructed mutants 2) DhaA31 (improved activity)[15] and 3) DhaA90R (increased enantioselectivity).[16] Kinetic models were built for pathways with each variant, and the enzyme stoichiometry was optimized under defined constraints.

We initially prepared soluble enzymes with purities of ≥95% for DhaA and EchA and ≥85% for HheC (Supporting Information). To validate the one-pot multienzyme biotransformation of TCP into GLY, 1 mg each of purified DhaA, HheC, and EchA were mixed in 10 mL of Tris-SO$_4$ buffer (pH 8.5) and incubated with 2 mM TCP at 37°C for 300 min. The enzymes have similar molecular weights (34.1, 29.3, and 36.5 kDa, respectively), so mass ratio roughly equals molar ratio. A GC method for detecting and quantifying TCP and all pathway intermediates in a single analysis was developed and used to monitor the five-step process (see the Experimental Section and Figure S1 in the Supporting Information). The time course for the conversion confirmed pathway viability and revealed two major bottlenecks: 1) conversion of TCP into 2,3-dichloropropan-1-ol (DCP), and 2) mismatched selectivity of DhaA and HheC, thus causing accumulation of (S)-DCP (Scheme 1 and Figure S2). Similar bottlenecks have been identified in vivo.[11]
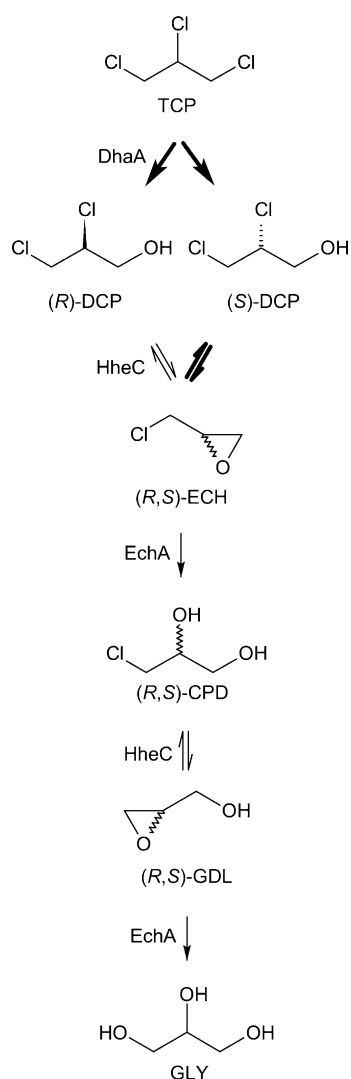
We then investigated two DhaA mutants with properties tuned to address these bottlenecks. DhaA31 was previously constructed in our laboratory by using computer-aided directed evolution of protein tunnels.[15] Its catalytic rate towards TCP is 32 times that of wild-type DhaA. Mutant DhaA90R was obtained by van Leeuwen and co-workers ("DhaAr5-90R") by

These are not the final page numbers! ↗↗

Scheme 1. Synthetic pathway for the three-enzyme biotransformation of 1,2,3-trichloropropane. Five consecutive steps are catalyzed by the haloalkane dehalogenase DhaA, from *Rhodococcus rhodochrous* NCIMB 13064, haloalcohol dehalogenase HheC from *Agrobacterium radiobacter* AD1, and epoxide hydrolase EchA from *Agrobacterium radiobacter* AD1. 1,2,3-trichloropropane (TCP) is converted via (R)- (S)-2,3-dichloropropane-1-ol (DCP), epichlorohydrin (ECH), 3-chloropropane-1,2-diol (CPD), and glycidol (GDL) to glycerol (GLY). Key bottlenecks are indicated by bold arrows.

Table 1. Experimental steady-state kinetic parameters in the kinetic model.			
DhaA		**HheC**	
$K_{m,TCP}$ [mM]	1.01 ± 0.08	$K_{m,(R)\text{-}DCP}$ [mM]	2.49 ± 0.16
$k_{cat,TCP,(R)\text{-}DCP}$ [s^{-1}]	$0.04^{[a]}$	$K_{m,(S)\text{-}DCP}$ [mM]	3.33 ± 0.51
$k_{cat,TCP,(S)\text{-}DCP}$ [s^{-1}]	$0.03^{[a]}$	$K_{m,CPD}$ [mM]	0.86 ± 0.07
DhaA31		$k_{cat,(R)\text{-}DCP}$ [s^{-1}]	1.81 ± 0.05
$K_{m,TCP}$ [mM]	1.79 ± 0.09	$k_{cat,(S)\text{-}DCP}$ [s^{-1}]	0.08 ± 0.00
$k_{cat,TCP,(R)\text{-}DCP}$ [s^{-1}]	$0.58^{[b]}$	$k_{cat,CPD}$ [s^{-1}]	2.38 ± 0.06
$k_{cat,TCP,(S)\text{-}DCP}$ [s^{-1}]	$0.47^{[b]}$	**EchA**	
DhaA90R		$K_{m,ECH}$ [mM]	0.09 ± 0.08
$K_{m,TCP}$ [mM]	12.56 ± 2.99	$K_{m,GDL}$ [mM]	3.54 ± 0.09
$k_{cat,TCP,(R)\text{-}DCP}$ [s^{-1}]	$0.19^{[c]}$	$k_{cat,ECH}$ [s^{-1}]	14.37 ± 0.52
$k_{cat,TCP,(S)\text{-}DCP}$ [s^{-1}]	$0.02^{[c]}$	$k_{cat,GDL}$ [s^{-1}]	3.96 ± 0.08

[a] Determined from the ratio of (R)- and (S)-DCP production as 56 and 44% of 0.07 ± 0.00 s^{-1} for $k_{cat,TCP,(R)\text{-}DCP}$ and $k_{cat,TCP,(S)\text{-}DCP}$ respectively (Supporting Information, Experimental Section). [b] Determined as 55 and 45% of 1.05 ± 0.02 s^{-1} for $k_{cat,TCP,(R)\text{-}DCP}$ and $k_{cat,TCP,(S)\text{-}DCP}$ respectively. [c] Determined as 90 and 10% of 0.21 ± 0.03 s^{-1} for $k_{cat,TCP,(R)\text{-}DCP}$ and $k_{cat,TCP,(S)\text{-}DCP}$ respectively.

focused directed evolution of DhaA31. It has the same activity as wild-type DhaA but seven times higher specificity for the (R)-DCP configuration.[16] Time courses for the three-enzyme conversion of TCP with purified DhaA31 or DhaA90R were recorded, as for the wild type. The differences between the resulting conversion profiles were consistent with the kinetic properties of DhaA, DhaA31, and DhaA90R (Figure S2 and Tables S2–S4).

Sixteen steady-state kinetic parameters were determined for the purified enzymes to establish a kinetic model of the pathway (Table 1 and the Supporting Information). All the studied reactions exhibited Michaelis–Menten kinetics. The conversion of glycidol (GDL) into GLY was described by a Michaelis–Menten equation, with two inhibition constants defining the inhibitory effects of GLY (product inhibition constant $K_i = 1.00$ mM) and TCP (shared equilibrium inhibition constant $K_c = 0.21$ mM; Supporting Information). These effects together with the substrate preference of EchA for epichlorohydrin (ECH) caused GDL accumulation (Figure S2).

The kinetic model was validated against experimental data for the three-enzyme conversion of 2 mM TCP (Figure S2). The two datasets were in good agreement: with 1:1:1 mixtures of the three enzymes (total 3 mg), the predicted (and measured) productivities of the DhaA, DhaA31, and DhaA90R pathways were 72% (62%), 85% (85%) and 45% (42%), respectively. No enzyme inactivation occurred, but the model could be extended to include inactivation constants if necessary.

The model was then used to predict the DhaA, HheC, and EchA loadings needed to achieve 95% conversion of TCP into GLY under the chosen conditions by simulating stepwise increases in enzyme loading within the reaction system until the productivity goal was reached (see the Experimental Section and the Supporting Information). At a DhaA/HheC/EchA mass ratio of 1:1:1, the wild-type haloalkane dehalogenase pathway reached the productivity goal with 2.4 mg of each enzyme (total 7.2 mg; Figure 1). The DhaA31 and DhaA90R pathways required 1.8 mg and 4 mg of each enzyme, respectively, (i.e., total enzyme loads of 5.4 and 12 mg) to reach the goal. The differences in the modeled time courses and quantities of enzyme required to achieve 95% conversion for the three pathway variants demonstrate the profound effects of introducing engineered DhaA variants (Figure 1). Despite pronounced accumulation of DCP and GDL during the initial 25 min, the DhaA31 pathway was around 25% more efficient than the wild-type version. DhaA31 significantly accelerated the conversion of TCP and thus accelerated the consumption of accumulated GDL by suppressing TCP's inhibitory effect. In contrast, DhaA90R reduced system efficiency despite effectively minimizing DCP accumulation. This selective but catalytically inefficient mutant was thus not beneficial.

These are not the final page numbers! ↗↗
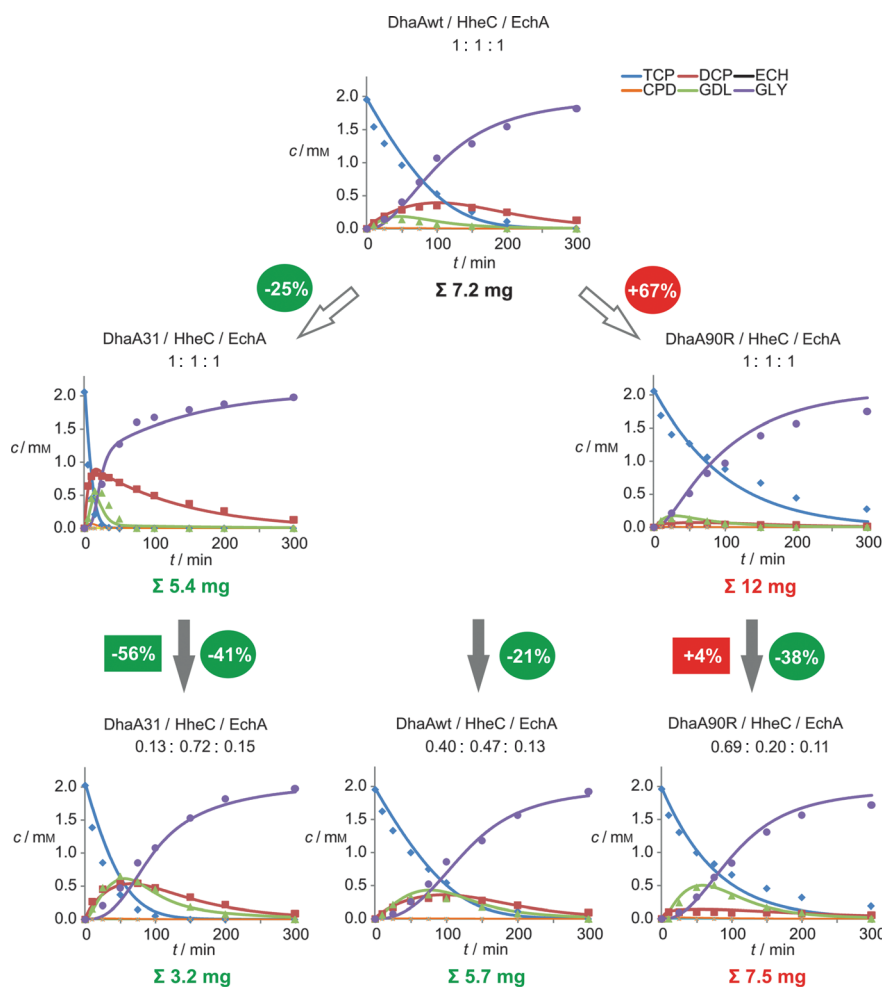
Figure 1. Optimization of three-enzyme conversion of 1,2,3-trichloropropane by kinetic modeling and employ-ment of engineered enzyme variants. Calculated and measured results are indicated by solid lines and symbols, respectively. The following parameters were constrained: reaction volume (10 mL), initial TCP concentration (2 mM), and reaction duration (300 min). The initial optimization goal was 95% conversion of TCP into GLY within 300 min by a 1:1:1 ratio (wild-type enzyme). The calculated and experimentally verified total enzyme loading (Σ) required to achieve this was 7.2 mg. The wild-type DhaA enzyme was then replaced with mutants DhaA31[23] or DhaA90R[24] to study the effect of their kinetics on the pathway (white arrows). Further optimization was achieved by tuning the enzyme ratios (gray arrows). Reductions in total enzyme loading achieved by employment of mu-tants or stoichiometry optimization alone and in combination are shown in circles and squares, respectively. Ex-perimental concentrations of TCP, DCP, ECH, CPD, and GDL were determined by GC. Concentrations of GLY were determined spectrophotometrically. Data points represent mean values from three independent experiments. (Error bars are omitted for clarity; standard deviations are provided in the Supporting Information; Tables S2–S4).

We then evaluated the effects of enzyme stoichiometry on efficiency. An algorithm was used to minimize the total enzyme load without sacrificing productivity (Experimental Section and Animation S1 in the Supporting Information). Opti-mal enzyme mass ratios were calculated for each pathway. The modeled time courses for individual reactions were similar in each case, but the optimized ratios and total enzyme loadings differed significantly between pathways (Figure 1). Enzyme stoichiometry optimization increased efficiency in the DhaA, DhaA31, and DhaA90R pathways and reduced the total enzyme loading required for > 95% conversion, by 21, 41, and 38%, respectively.

All optimization simulations were validated by testing the enzyme mass ratios in vitro. The resulting data agreed very

closely with the predictions (Figure 1). The optimized DhaA90R pathway was around 10% less productive than pre-dicted, possibly because the K_m of DhaA90R for TCP was under-estimated due to the limited water solubility of TCP (~ 10 mM). In all other cases, the optimized systems achieved pro-ductivities of 94–98% (Ta-bles S2–S4). Because the experi-mental time courses only reflect optimal cases based on prede-fined constraints, we used the simulated data to create 3D iso-productivity charts to show the effects of varying the loadings of DhaA variant, HheC, and EchA (Figure 2). These show the limit-ing components for each path-way and can be used to identify solutions with similar productivi-ties.

Our results demonstrate that both modifying enzyme kinetic parameters and optimizing enzyme stoichiometry improved the efficiency of the studied multienzyme system. However, the far simpler process of stoi-chiometry optimization had a greater impact than introducing engineered enzymes. The opti-mized pathway using wild-type DhaA required a similar total enzyme load to the non-opti-mized pathway using the engi-neered DhaA31 (5.7 vs. 5.4 mg), thus showing that kinetic model-ing alone can provide excellent solutions in certain cases. Natu-rally, the best result was ach-ieved with an optimized pathway using engineered DhaA31: additive effects in this case reduced the catalyst load required for 95% productivity by 56% relative to the unoptimized wild-type pathway (Figure 1). This would be very economically ben-eficial in a large-scale industrial process.

In summary, we present experimentally validated in silico op-timization of a multienzyme process by biocatalyst stoichiome-try tuning. Our workflow entails 1) experimental verification of process viability, 2) determination of enzyme kinetics, 3) iden-tification of pathway bottlenecks and selection of suitable en-gineered enzymes, 4) development of a robust and accurate ki-netic model, 5) experimental model validation, and 6) process optimization by in silico enzyme stoichiometry modeling. Recent progress in efficient enzyme stabilization[17] and ex vivo

These are not the final page numbers! ↗↗
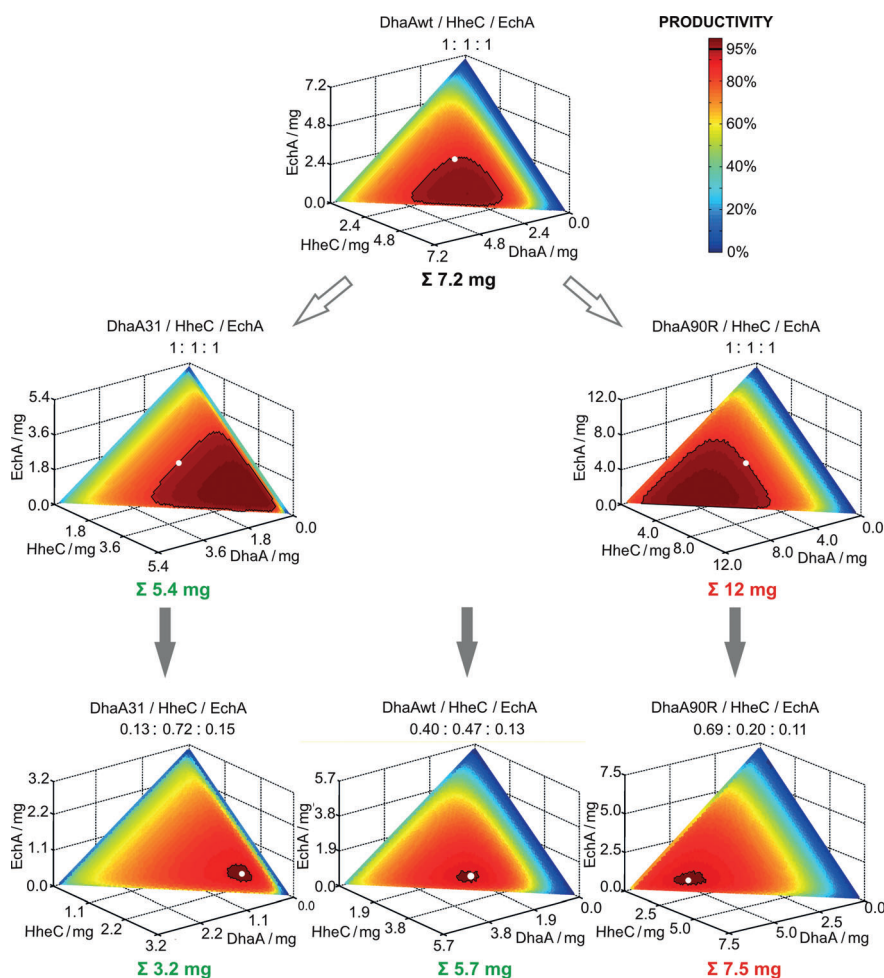
Figure 2. Isoproductivity color charts showing how biocatalyst concentration affects productivity in the three-enzyme conversion of 1,2,3-trichloropropane into glycerol. Applied constraints are as in Figure 1; the optimal solutions in each figure are indicated by white dots. Values on axes represent the loading of the corresponding enzyme in the reaction mixture. The black line indicates the threshold productivity (95%).

Python 2.7 (Software S1 in the Supporting Information). The equations were expressed in differential form and integrated by using Euler's method (step size, 0.18 s). The effects of using different DhaA variants on the performance of the multienzyme process were evaluated with the following constraints: at least 95% conversion of TCP into GLY was to be achieved within 300 min when using DhaA variant, HheC, and EchA in an unoptimized mass ratio (1:1:1) at a total enzyme loading of 3.0 mg. The optimization algorithm increased the total enzyme loading in a stepwise fashion, by using increments of around 0.1 mg (i.e., increasing the loading of each individual enzyme by 0.066 mg in each step) until 95% conversion was surpassed. The enzyme stoichiometry in each of three pathways was then optimized to identify the DhaA variant/HheC/EchA ratio that would yield 95% conversion of 2 mM TCP into GLY within 300 min while minimizing the combined loading of the three enzymes. The algorithm searched for the most efficient ratio of three enzymes in the system starting with a total enzyme loading of 3 mg. The total enzyme loading within the system was increased in 0.1 mg increments until the most efficient ratio surpassed 95% conversion. For each total enzyme loading, 496 enzyme ratios were evaluated with step of 3% of a given total amount.

cofactor regeneration[18] together with the development of integrated analytical techniques,[19] increases in computational power, and the growing availability of kinetic data, will enable the refinement of many useful biotransformations. We believe that the workflow described herein and implemented in the provided computer code (Supporting Information) represents a widely applicable strategy for rapid optimization of multienzyme processes.

Experimental Section

Computational optimization of the multienzyme conversion of TCP: The initial constraints in modeling multienzyme conversion of TCP (to verify the developed kinetic model) were as follows: TCP starting concentration 2 mM (initial experimental concentration as close to 2 mM as possible; Tables S2–S4); the multienzyme reaction was allowed to proceed for 300 min; the concentration of each enzyme (DhaA variant, HheC, and EchA) was 0.1 mg mL^{-1} (total enzyme loading in 10 mL, 3 mg). Dynamic simulations of the multienzyme system based on a series of Michaelis–Menten equations (Supporting Information) were performed by using code written in

Multienzyme conversion of TCP in batch experiments: The multienzyme conversion of TCP (2 mM) was assayed in Tris-SO$_4$ buffer (10 mL, 50 mM, pH 8.5) in 25 mL micro-flasks sealed with Mininert valves (Alltech, USA) at 37 °C. The reaction was initiated by adding a defined amounts of purified DhaA variant, HheC, and EchA. Samples were periodically taken, mixed 1:1 with acetone containing hexanol (4 mM) as an internal standard, and analyzed by GC to determine the concentrations of TCP, DCP, ECH, CPD, and GDL (Supporting Information). Selected samples were analyzed by GC-MS to verify the identities of the metabolites. The concentration of GLY in the reaction mixture was determined spectrophotometrically by using the Free Glycerol Assay Kit (BioVision, Milpitas, CA). Details are provided in the Supporting Information.

Acknowledgements

These are not the final page numbers! ↗↗

[1] a) I. Ardao, E. T. Hwang, A.-P. Zeng, *Adv. Biochem. Eng./Biotechnol.* **2013**, *137*, 153; b) Z. Findrik, D. Vasić-Rački, *Chem. Biochem. Eng. Q.* **2009**, *23*, 545; c) P. A. Santacoloma, G. Sin, K. V. Gernaey, J. M. Woodley, *Org. Process Res. Dev.* **2011**, *15*, 203; d) S. Schoffelen, J. C. M. van Hest, *Curr. Opin. Struct. Biol.* **2013**, *23*, 613.

[2] N. Ishii, Y. Suga, A. Hagiya, H. Watanabe, H. Mori, M. Yoshino, M. Tomita, *FEBS Lett.* **2007**, *581*, 413.

[3] Z. Findrik, D. Vasić-Rački, *Biotechnol. Bioeng.* **2007**, *98*, 956.

[4] A. Itoh, Y. Ohashi, T. Soga, H. Mori, T. Nishioka, M. Tomita, *Electrophoresis* **2004**, *25*, 1996.

[5] I. Ardao, A.-P. Zeng, *Chem. Eng. Sci.* **2013**, *87*, 183.

[6] a) F. Lopez-Gallego, C. Schmidt-Dannert, *Curr. Opin. Chem. Biol.* **2010**, *14*, 174; b) A. Meyer, R. Pellaux, S. Panke, *Curr. Opin. Microbiol.* **2007**, *10*, 246; c) S. Billerbeck, J. Härle, S. Panke, *Curr. Opin. Biotechnol.* **2013**, *24*, 1037.

[7] a) A. S. Bommarius, J. K. Blum, M. J. Abrahamson, *Curr. Opin. Chem. Biol.* **2011**, *15*, 194; b) U. T. Bornscheuer, G. W. Huisman, R. J. Kazlauskas, S. Lutz, J. C. Moore, K. Robinson, *Nature* **2012**, *485*, 185.

[8] a) D. G. Blackmond, *Angew. Chem. Int. Ed.* **2005**, *44*, 4302; *Angew. Chem.* **2005**, *117*, 4374; b) R. Xue, J. M. Woodley, *Bioresour. Technol.* **2012**, *115*, 183.

[9] W. Van Hecke, A. Bhaqwat, R. Ludwig, J. Dewulf, D. Haltrich, H. Van Langenhove, *Biotechnol. Bioeng.* **2009**, *102*, 1475.

[10] G. Samin, D. B. Janssen, *Environ. Sci. Pollut. Res. Int.* **2012**, *19*, 3067.

[11] a) T. Bosma, E. Kruizinga, E. J. de Bruin, G. J. Poelarends, D. B. Janssen, *Appl. Environ. Microbiol.* **1999**, *65*, 4575; b) T. Bosma, J. Damborský, G. Stucki, D. B. Janssen, *Appl. Environ. Microbiol.* **2002**, *68*, 3582; c) N. P. Kurumbang, P. Dvorak, J. Bendl, J. Brezovsky, Z. Prokop, J. Damborsky, *ACS Synth. Biol.* **2014**, *3*, 172.

[12] A. N. Kulakova, M. J. Larkin, L. A. Kulakov, *Microbiology* **1997**, *143*, 109.

[13] J. E. T. van Hylckama Vlieg, L. Tang, J. H. Lutje Spelberg, T. Smilda, G. J. Poelarends, T. Bosma, A. E. J. van Merode, M. W. Fraaije, D. B. Janssen, *J. Bacteriol.* **2001**, *183*, 5058.

[14] R. Rink, M. Fennema, M. Smids, U. Dehmel, D. B. Janssen, *J. Biol. Chem.* **1997**, *272*, 14650.

[15] M. Pavlova, M. Klvana, Z. Prokop, R. Chaloupkova, P. Banas, M. Otyepka, R. C. Wade, M. Tsuda, Y. Nagata, J. Damborsky *Nat. Chem. Biol.* **2009**, *5*, 727.

[16] J. G. van Leeuwen, H. J. Wijma, R. J. Floor, J.-M. van der Laan, D. B. Janssen, *ChemBioChem* **2012**, *13*, 137.

[17] a) T. Koudelakova, R. Chaloupkova, J. Brezovsky, Z. Prokop, E. Sebestova, M. Hesseler, M. Khabiri, M. Plevaka, D. Kulik, I. Kuta Smatanova, P. Rezacova, R. Ettrich, U. T. Bornscheuer, J. Damborsky, *Angew. Chem. Int. Ed.* **2013**, *52*, 1959; *Angew. Chem.* **2013**, *125*, 2013; b) M. T. Reetz, J. D. Carballeira, A. Vogel, *Angew. Chem. Int. Ed.* **2006**, *45*, 7745; *Angew. Chem.* **2006**, *118*, 7909.

[18] a) L. Lauterbach, O. Lenz, K. A. Vincent, *FEBS J.* **2013**, *280*, 3058; b) R. A. Scism, B. O. Bachmann, *ChemBioChem* **2010**, *11*, 67.

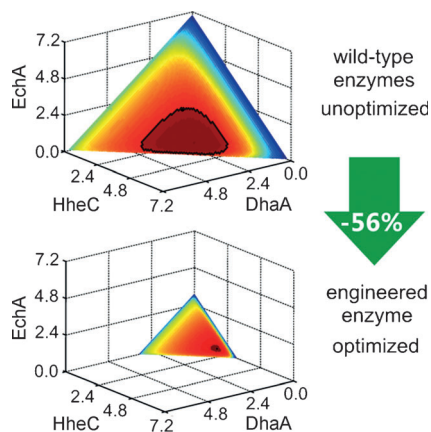[19] M. Bujara, M. Schümperli, R. Pellaux, M. Heinemann, S. Panke, *Nat. Chem. Biol.* **2011**, *7*, 271.

These are not the final page numbers! ↗↗

COMMUNICATIONS

P. Dvorak, N. P. Kurumbang, J. Bendl,
J. Brezovsky, Z. Prokop, J. Damborsky*

■■ – ■■

**Maximizing the Efficiency of
Multienzyme Process by Stoichiometry
Optimization**

Recipe for success: We propose a workflow for optimizing complex multienzyme reactions by kinetic modeling and stoichiometry optimization. By using a three-enzyme system catalyzing a five-step chemical conversion we show that selection of suitable enzymes and stoichiometry optimization can greatly reduce biocatalyst loadings. This work highlights the potential of kinetic modeling for optimizing industrial biocatalytic processes.

These are not the final page numbers! ↗↗